Proceedings of the International Conference on Oxide Materials for Electronic Engineering (OMEE 2021)

Synthesis and Luminescence Properties of Pure and Doped with Europium(III) $K_{0.45}Bi_{0.55}Mo_{0.9}V_{0.1}O_4$ Solid Solutions

V.P. Chornii[a,b,*], V.V. Boyko[a], S.G. Nedilko[b], O.V. Petrenko[b], V.M. Prokopets[b], K.V. Terebilenko[b] and M.S. Slobodyanyk[b]

[a] *National University of Life and Environmental Sciences of Ukraine, 15 Geroiv Oborony str., 03041 Kyiv, Ukraine*
[b] *Taras Shevchenko National University of Kyiv, 64/13 Volodymyrska str., 01301 Kyiv, Ukraine*

Doi: 10.12693/APhysPolA.141.237 *e-mail: vchornii@gmail.com

The results of synthesis, crystal structure characterization, and luminescence properties study of pure and Eu^{3+}-doped $K_{0.45}Bi_{0.55}Mo_{0.9}V_{0.1}O_4$ solid solutions have been reported. The obtained powders crystallize in a compact form with an average size of the particles of about 5–10 μm. It was found that doping with europium leads to the transformation of the host from monoclinic to tetragonal scheelite-like phase. The Eu^{3+}-doped samples reveal intensive red luminescence under excitation in ultraviolet and blue spectral regions. Energy transfer from molybdate–vanadate host to Eu^{3+} ions takes place in the studied solid-solution. Intensity of the red luminescence increases when Eu^{3+} content increases and no concentration quenching has been found.

topics: bismuth, europium, luminescence, molybdate

1. Introduction

Bismuth-containing molybdate and vanadate compounds are of great interest due to the prospects for their application as laser active media, phosphors, scintillating and photocatalytic materials, pigments, etc. [1–4]. The variety of applications is related to their capability to effectively absorb incident light in ultraviolet and blue spectral regions due to electronic transitions in BiO_x polyhedra and MoO_4 or VO_4 tetrahedra. The electronic states of Bi, Mo (or V), and O determine the electronic structure of such compounds near the edges of valence and conduction bands [5, 6]. The bismuth as a regular element in the compounds plays two roles: (i) band of $6s \rightarrow 6p$ electronic transitions in Bi^{3+} cations located in UV or blue spectral region improving host absorption, and (ii) the Bi^{3+} can be substituted by RE^{3+} ions easily because of their similar ionic radii and the same charge states. A similar situation takes place for mixed-anion compounds containing both MoO_4 and VO_4 groups. Importantly, substituting molybdenum with vanadium allows decreasing of the band gap values, which results in shifting the absorption band to longer wavelengths [7]. This shifting allows combining direct and host-related photoluminescence (PL) excitation of the RE ions in the case of molybdate–vanadate compounds doped with rare-earth (RE) ions. Consequently, better effectiveness of PL excitation can be achieved, which is necessary for the elaboration of phosphor materials.

Synthesis and luminescence properties of the pure and Eu^{3+}-doped $K_{0.5x}Bi_{1-0.5x}(Mo_xV_{1-x})O_4$ solid solutions are reported in this paper. A key feature of such a crystal structure is the random distribution of K and Bi atoms over the same crystallographic positions, while Mo and V are more likely to be found in slightly distorted tetrahedra. Although both extreme cases, $KBi(MoO_4)_2$ and $BiVO_4$, possess scheelite-like crystal structures, the former is monoclinic, while the latter is tetragonal. Our previous studies of the $K_{0.5x}Bi_{1-0.5x}(Mo_xV_{1-x})O_4$ system had shown that structural transformations take place upon a change in molybdenum to vanadium ratio. In particular, for $x = 0.1$–0.3 only a tetragonal phase was observed, while only a monoclinic phase was found for $x = 0.5$–0.9 [8]. Interestingly, the $A_{0.5x}Bi_{1-0.5x}(Mo_xV_{1-x})O_4$ (where A = Li, Na) solid solutions have tetragonal scheelite-like crystal structure for x above 0.1 [9, 10]. Such difference with the case of potassium can be ascribed to the difference in ionic radii and coordination number of these alkali metals in the molybdate–vanadate systems.

2. Experimental details

Synthesis of the undoped and Eu^{3+}-doped $K_{0.45}Bi_{0.55}Mo_{0.9}V_{0.1}O_4$ samples was performed by solid state technique. Analytically pure A_2CO_3, Bi_2O_3, MoO_3, V_2O_5, and Eu_2O_3 were taken as starting materials without further purification. Stoichiometric amounts of the reagents were thoroughly mixed in an agate mortar into fine powders. At the first stage, the mixtures have been calcinated at 550°C for 2 h to get rid of carbon dioxide. Then, the resulting powders were mixed with a drop of ethanol, thoroughly reground, and sintered at 600°C for 5 h, 700°C for 8 h, and 750°C for 8 h with intermediate regrinding after each temperature in covered alumina crucibles.

Phase composition has been investigated by powder XRD using of Shimadzu XRD-6000 diffractometer (curved pyrolytic graphite counter monochromator, CuK_α radiation with $\lambda = 1.54184$ Å) operating in Bragg–Brentano ($\Theta/(2\Theta)$) geometry ($2\Theta = 5$–$70°$).

SEM images were obtained on JEOL JSM 6060 LV for the polycrystalline samples coated with gold.

The photoluminescence (PL) studies under excitations in the UV and visible regions were carried out at room temperature. The diffraction spectrometer MDR-23 was used to register the PL emission and excitation spectra. The radiation of the Xenon-arc lamp (150 W) was used for the PL excitation. All the spectra were corrected on the system response.

3. Results and discussion

3.1. X-ray diffraction study

The solid solutions as x $(K_{0.5}Bi_{0.5}MoO_4)$ $-(1-x)$ $BiVO_4$ are related to the $CaWO_4$ scheelite structure and crystallize in tetragonal symmetry with the space group $I4_1/a$. The parent structure is build up from CaO_8 dodecahedra and MoO_4 tetrahedra. Multiple substitutions within cationic and anionic sublattices in the case of titled solid solutions lead to the formation of mixed $(Mo/V)O_4$ tetrahedra and $(K/Bi)O_8$ polyhedra. To maintain the scheelite framework, $(K/Bi)O_8$ polyhedra should share an edge, whereas $(Mo/V)O_4$ tetrahedra are isolated from each other. Each $(Mo/V)O_4$ tetrahedron shares a corner with $(K/Bi)O_8$ polyhedra. Mainly cationic and anionic substitution leads to a random distribution of V/Mo and metals in a dodecahedral environment [11]. The possibility of symmetry change is often discussed in light of XRD patterns. The X-ray diffraction pattern for solid solution $K_{0.45}Bi_{0.55}Mo_{0.9}V_{0.1}O_4$ sintered at 750°C is presented in Fig. 1. As could be expected from previously reported data [12], the solid solution containing 10 mol% of molybdenum crystallizes in a monoclinic scheelite-like structure. The lowering of symmetry is confirmed by the splitting of several

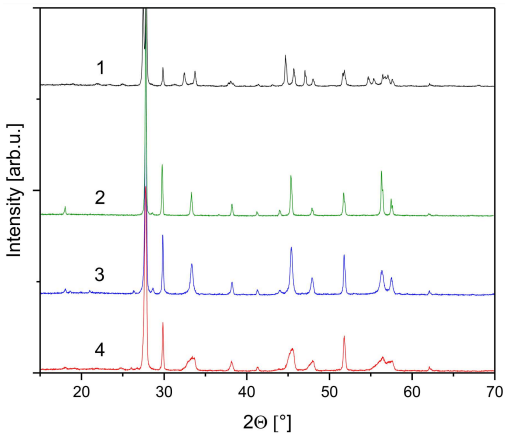

Fig. 1. X-ray diffraction (XRD) patterns for $K_{0.45}Bi_{0.55-y}Eu_yMo_{0.9}V_{0.1}O_4$ samples, $y = 0$ (1), 0.05 (2), 0.10 (3) and 0.15 (4).

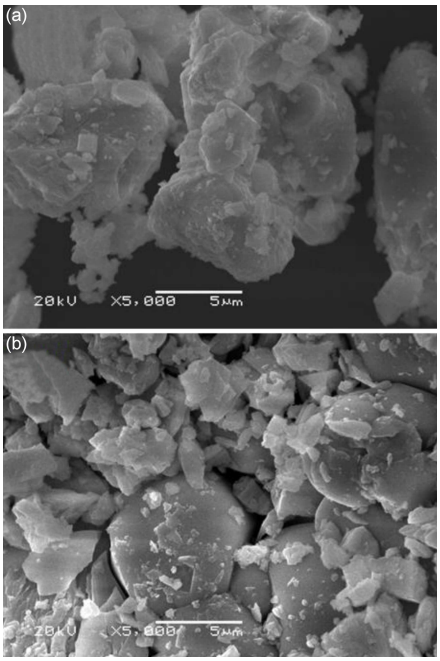

Fig. 2. SEM images of $K_{0.45}Bi_{0.55}Mo_{0.9}V_{0.1}O_4$ and $K_{0.45}Bi_{0.40}Eu_{0.15}Mo_{0.9}V_{0.1}O_4$ samples.

reflection peaks, such as the 28.2 of 2Θ reflection, which is attributed to (101) peak in tetragonal systems splitting into (101) and (011) peaks in the case of monoclinic $K_{0.45}Bi_{0.55}Mo_{0.9}V_{0.1}O_4$. Analogously, the (200) peak at 32.8 of 2Θ is splitting into (200) and (020) peaks (Fig. 1, curve 1). In the case of Eu-doping, the symmetry of solid solutions obtained is tetragonal (Fig. 1, curves 2–4). There is no splitting observed for $K_{0.45}Bi_{0.55-y}Eu_yMo_{0.9}V_{0.1}O_4$ in the case of $y = 0.05$–0.15. This peculiarity has been identified for the first time and can be explained by common coordination requirements of Ca^{2+}, Bi^{3+}, and Eu^{3+} cations. Moreover, pure europium-containing scheelite-related molybdates crystallize in the $I4_1/a$ space group [13, 14].

3.2. Scanning electron microscopy

The SEM images of $K_{0.45}Bi_{0.55}Mo_{0.9}V_{0.1}O_4$ and $K_{0.45}Bi_{0.40}Eu_{0.15}Mo_{0.9}V_{0.1}O_4$ samples are shown in Fig. 2. The powder is crystallized in a compact form with well separated particles of an average size of about 5–10 μm. A grain boundary between the microcrystals is clearly seen after annealing at 750°C. Both pure and doped with europium samples are characterized by irregularly shaped particles, which develop loose agglomerates (Fig. 2).

3.3. Luminescence spectroscopy

The undoped $K_{0.5x}Bi_{1-0.5x}Mo_xV_{1-x}O_4$ solid solutions do not reveal any significant luminescence at room temperature when excited in 250–500 nm spectral range. This situation occurs because of the strong temperature quenching of photoluminescence, which is typical for many molybdate and vanadate compounds [15–17]. The luminescence signal of the undoped samples can be easily registered at $T = 77$ K. However, increasing the vanadium content leads to a decrease in the total PL intensity. The main bands in PL excitation spectra of $K_{0.5x}Bi_{1-0.5x}Mo_xV_{1-x}O_4$ samples have maxima near 320, 375, and 410 nm and can be ascribed to processes in regular MoO_4, defective MoO_4, and VO_4 molecular anions, respectively (detailed analysis of PL emission and excitation for can be found in [8]).

The Eu^{3+} doped samples reveal intensive, even at room temperature, PL related with $^5D_0 \rightarrow {}^7F_{J=1-4}$ electronic transitions in these RE ions under excitation both in absorption bands of molybdate–vanadate host and absorption under f–f intrinsic transitions in Eu^{3+} ions (Fig. 3). Interestingly, the number and intensity of the PL bands depend on the type of excitation.

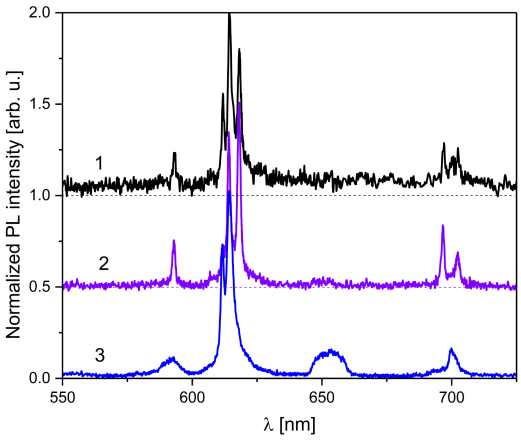

Fig. 3. Photoluminescence spectra of $K_{0.45}Bi_{0.40}Eu_{0.15}Mo_{0.9}V_{0.1}O_4$ solid solution obtained for excitation at $\lambda_{ex} = 320$ nm (1), 396 nm (2) and 473 nm (3) at room temperature. Zero intensity levels for spectra 1 and 2 are shown by dashed lines.

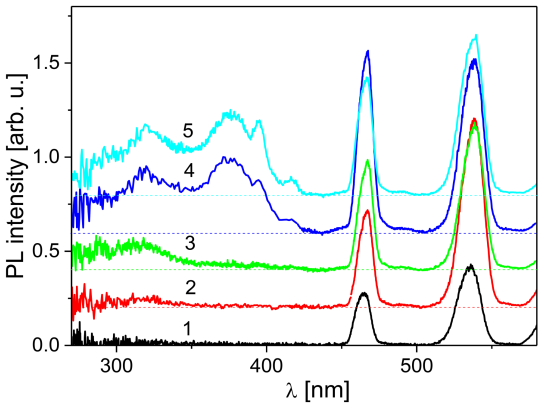

Fig. 4. Photoluminescence excitation spectra of the $K_{0.45}Bi_{0.55-y}Eu_yMo_{0.9}V_{0.1}O_4$ samples, where $y = 0.01$ (1), 0.02 (2), 0.05 (3), 0.10 (4) and 0.15 (5), $\lambda_{em} = 614.4$ nm, $T = 300$ K. Zero intensity levels for spectra 2–5 are shown by dashed lines.

The PL excitation spectra for the $K_{0.45}Bi_{0.55-y}Eu_yMo_{0.9}V_{0.1}O_4$ samples are shown in Fig. 4. Only bands near 470 and 538 nm that correspond to absorption transitions in Eu^{3+} ions from ground electronic state $^7F_0$ to $^5D_2$ and $^5D_1$ excited states, respectively, have been measured in the case of the lowest europium concentration. The relatively narrow band near 396 nm that corresponds to $^7F_0 \rightarrow {}^5L_6$ electronic transition in Eu^{3+} ions was observed when the content of Eu^{3+} ions increased (y value in Fig. 4, curves 4 and 5). The weak band with a maximum near 320 nm was also observed, starting from $y = 0.02$. One more wide band with a maximum near 375 nm was observed when europium content reached $y = 0.10$. These bands can be ascribed to light absorption processes in MoO_4 molecular anions, as was stated earlier [8]. Undoubtedly, described data is a manifestation of energy transfer from molybdate–vanadate host to Eu^{3+} ions.

The changes in PL intensity for the set of $K_{0.45}Bi_{0.55-y}Eu_yMo_{0.9}V_{0.1}O_4$ samples were studied for the case of PL excitation at 473 nm (Fig. 5). The difference in the shape of the bands in PL spectra for the samples with different concentrations of Eu^{3+} ions can be seen only in the region of $^5D_0 \rightarrow {}^7F_3$ and $^5D_0 \rightarrow {}^7F_4$ transitions. Bands of these transitions have little practical interest as those with low intensity and as located at the region of the low sensitivity of the human eye. However, from the viewpoint of phosphor application, the bands of $^5D_0 \rightarrow {}^7F_1$ and $^5D_0 \rightarrow {}^7F_2$ transition should be considered. The total intensity in the region 550–725 nm and intensities of bands of $^5D_0 \rightarrow {}^7F_1$ and $^5D_0 \rightarrow {}^7F_2$ transitions (calculated as the area under spectra in 580–600 and 600–630 nm range, respectively) are collected in Table I. As can be seen, no concentration quenching was observed for the studied content of Eu^{3+}

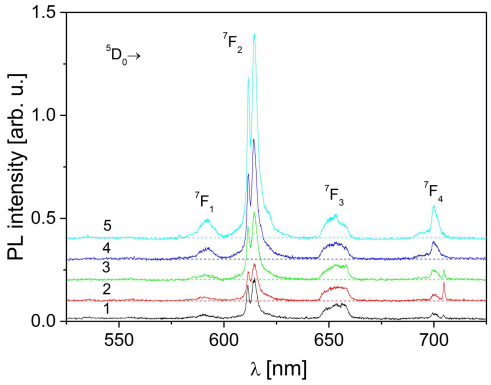

Fig. 5. Photoluminescence emission spectra of $K_{0.45}Bi_{0.55-y}Eu_yMo_{0.9}V_{0.1}O_4$ samples, where $y = 0.01$ (1), 0.02 (2), 0.05 (3), 0.10 (4) and 0.15 (5), obtained for excitation at $\lambda_{ex} = 473$ nm, $T = 300$ K. Zero intensity levels for spectra 2–5 are shown by dashed lines.

TABLE I

Intensities of photoluminescence bands and asymmetry ratio for the $K_{0.45}Bi_{0.55-y}Eu_yMo_{0.9}V_{0.1}O_4$ samples, calculated for PL excitation at $\lambda_{ex} = 473$ nm, $T = 300$ K.

y	I_{total} [arb.u.]	$I(^5D_0 \rightarrow {}^7F_1)$ [arb.u.]	$I(^5D_0 \rightarrow {}^7F_2)$ [arb.u.]	R
0.01	0.36	0.031	0.146	4.7
0.02	0.27	0.020	0.128	6.4
0.05	0.48	0.037	0.252	6.8
0.10	0.72	0.070	0.403	5.8
0.15	1.00	0.100	0.672	6.7

in $K_{0.45}Bi_{0.55-y}Eu_yMo_{0.9}V_{0.1}O_4$. In order to estimate the local symmetry of Eu^{3+} ions in various compounds, the asymmetry ratios

$$R = \frac{I(^5D_0 \rightarrow {}^7F_2)}{I(^5D_0 \rightarrow {}^7F_1)} \quad (1)$$

were calculated. It is well known that R values above 1 correspond to the non-centrosymmetric local surrounding of europium [18].

4. Conclusions

The samples of pure and Eu^{3+}-doped $K_{0.45}Bi_{0.55}Mo_{0.9}V_{0.1}O_4$ solid solutions were obtained by solid state technique, in the form of microcrystalline powders with grain sizes about 5–10 μm. The crystal structure transformation of the $K_{0.45}Bi_{0.55}Mo_{0.9}V_{0.1}O_4$ to more symmetrical occurs when doped with europium.

The undoped $K_{0.45}Bi_{0.55}Mo_{0.9}V_{0.1}O_4$ samples do not reveal luminescence at room temperature, while Eu^{3+}-doped samples are characterized by intensive red luminescence when PL excitation takes place in ultraviolet or blue spectral regions. The intensity of red luminescence increases with increase of Eu^{3+} content, and no concentration quenching was found.

References

[1] M. Rico, A. Méndez-Blas, V. Volkov, M.Á. Monge, C. Cascales, C. Zaldo, A. Kling, M.T. Fernández-Díaz, *J. Opt. Soc. Am. B* **23**, 2066 (2006).

[2] F. Baur, T. Jüstel, *Opt. Mater. X* **1**, 100015 (2019).

[3] V. Manikandan, M.A. Mahadik, I.S. Hwang, W.S. Chae, J. Ryu, J.S. Jang, *ACS Omega* **6**, 23901 (2021).

[4] D. Poda, *Physics* **3**, 473 (2021).

[5] A. Walsh, Y. Yan, M.N. Huda, M.M. Al-Jassim, S.H. Wei, *Chem. Mater.* **21**, 547 (2009).

[6] Y. Hizhnyi, S.G. Nedilko, V. Chornii, T. Nikolaenko, I.V. Zatovsky, K.V. Terebilenko, R. Boiko, *Solid State Phenom.* **200, 114 (2013)**.

[7] S.G. Nedilko, O. Chukova, V. Chornii, V. Degoda, K. Bychkov, K. Terebilenko, M. Slobodyanik, *Radiat. Meas.* **90**, 282 (2016).

[8] K. Terebilenko, S. Nedilko, O. Petrenko, M. Slobodyanik, V. Chornii, *Ukr. Chem. J.* **86**, 3 (2020).

[9] D. Zhou, L.X. Pang, H. Wang, J. Guo, X. Yao, C.A. Randall, *J. Mater. Chem.* **21**, 18412 (2011).

[10] D. Zhou, L.X. Pang, W.G. Qu, C.A. Randall, J. Guo, Z.M. Qi, T. Shao, X. Yao, *RSC Adv.* **3**, 5009 (2013).

[11] D. Zhou, L.X. Pang, Z.M. Qi, *Inorg. Chem.* **53**, 9222 (2014).

[12] D. Zhou, L.X. Pang, J. Guo, H. Wang, X. Yao, C. Randall, *Inorg. Chem.* **50**, 12733 (2011).

[13] P. Gall, P. Gougeon, *Acta Crystallogr. E Struct. Rep. Online* **62**, i120 (2006).

[14] J. Kim, *Inorg. Chem.* **56**, 8078 (2017).

[15] H. Ronde, G. Blasse, *J. Inorg. Nucl. Chem.* **40**, 215 (1978).

[16] O. Chukova, S.G. Nedilko, S.A. Nedilko, T. Voitenko, O. Gomenyuk, V. Sheludko, *Solid State Phenom.* **230**, 153 (2015).

[17] Y.A. Hizhnyi, S.G. Nedilko, V.P. Chornii, M.S. Slobodyanik, I.V. Zatovsky, K.V. Terebilenko, *J. Alloys Compd.* **614**, 420 (2014).

[18] R. Reisfeld, E. Zigansky, M. Gaft, *Mol. Phys.* **102**, 1319 (2004).